

Mechanical and Spectroscopic Investigations of Cr₂O₃ doped Calcium Aluminium Silicate Glasses

Kodumuri Veerabhadra Rao^{1,2*}, Padala Ashok¹, B. Appa Rao¹

¹Department of Physics, University College of Science, Osmania University, Hyderabad – 500 007, Telangana, INDIA

²Department of Physics, Humanities and Science, Methodist College of Engineering and Technology, Osmania University, Abids – 500 001, Telangana, INDIA

E-mail: veerabadhraraokodumuri@gmail.com

Mobile No.: +91 9346648223

Address for Postal Correspondance: Asst. Professor of Humanities and Science, Methodist College of Engineering and Technolgy, ABIDS, Hyderabad– 500 001, Telangana, INDIA

Abstract

The Cr³⁺ ions of silicate host glass is noteworthy for optical use, and which are useful as spectroscopic diode lasers in various electronic industrial applications. However, the available optical resource, which include different elastic and solid state electronic materials, need some refinement in their elastic structure, and spectroscopic properties towards development of advanced solid state LED's. In this view, the elastically flexible and optically efficient resource of chemical composition 60SiO₂+30Al₂O₃+(10-x)CaO:xCr₂O₃ has planned for synthesis followed by elastic, optical absorption and photoluminescence characterization. The materials developed are showing glassy behavior, and which was confirmed by the X-Ray diffraction. Physical properties of glasses are studied. Mechanical properties of glasses studied by means of measuring ultrasonic velocities. Which suggest materials of present kind are mechanically flexible. Optical absorption spectra of glasses is recorded, and which helps to calculate the Racah parameters of glasses. Refractive index, optical band edge, identified, and band gap also calculated. The Peak half width maximum, emissive cross-section, and transition probability of glasses evaluated with the help of photoluminescence characterization. This suggests glasses embedded with Cr³⁺ ions are photonic and with suitable excitation. All the results from the various characterization of glasses which include physical, mechanical, optical absorption, and photoluminescence results suggest a glass with 0.8 mol% Cr₂O₃ concentration is a helpful in mechanical, optical absorption, and photoluminescence results resource.

Keywords

SiO₂-Al₂O₃-CaO glasses; Physical Properties; Mechanical Properties; Optical absorption; Photoluminescence;

1. Introduction

Naturally, SiO₂ glasses are highly translucent, mechanically hard, and thermally stable. Their rich properties, such as density, refractive index, micro hardness, and optical transmittance will make them needful spectroscopic and W-LED host applications [1]. Since many years to present,

there have been wide-ranging research on a glasses with SiO₂ chemical constitutes due to their rich physical, mechanical and spectroscopic results [2]. The aluminium oxide is not a conventional glass former, but add-on Al₂O₃ to the glasses with SiO₂ improves their elastic nature, thermal stability, non-corrosion properties [3]. And also increase of Al₂O₃ in the SiO₂ glass host lead to more microhardness and thermal stability. SiO₂ embedded with Al₂O₃ glasses have a high order of optically stimulated luminescence, which will useful in various photoluminescence applications [4]. The addition of CaO to the pure silicate host enhances the refractive index, reduces the glass discoloration, and improves glass resource optically inert. Calcium silicate glass materials embedded with transition metal oxides are the most favourable candidates in the current semiconducting sectors and finds plentiful usage in the area of physical, mechanical, and spectroscopic applications [5]. Al₂O₃ also influence Si⁴⁺ ions in the lattice to change the strength, chemical endurance, mechanical and spectroscopic properties to a considerable extent of the overall glass network [6]. The CaO in silicate glass host stimulates Cr³⁺ ions for better optical output. The metal oxide Cr₂O₃ is a good nucleation agent, which involves divalent oxidation states in silica glass matrix to enhance physical, mechanical and spectroscopic properties [7]. Usually, Cr³⁺ ions have a substantial effect on the glass lattice, further which lead to advances in physical, mechanical, optical absorption, and photoluminescence properties of glass materials [8]. The glass with silicon dioxide chemical constitutes enclosing mixed valence states of Cr³⁺ ions are of recent interest as a thermoluminescent and cathode resource in rechargeable batteries as of their abnormal energy density, capacitance [9]. Subsequently, in the existing work, Cr₂O₃ doped aluminium silicate materials were synthesized and report for their suitability regarding elastic and spectroscopic behaviour [10]. Potential functions such as physical, mechanical, optical absorption and photoluminescence, etc., are achievable by improving tremendously advantageous solid-state luminescent glass resource that have captivated extensive attention. Because of this, the current research aimed to prepare solid-state glass materials of chemical composition 60SiO₂+30Al₂O₃+(10-x)CaO:xCr₂O₃ and to study the Cr³⁺ ionic influence on elastic, and spectroscopic behaviour of calcium alumina silicate glasses.

2. Experimental Methods

The oxides in mol% of 60SiO₂+30Al₂O₃+(10-x)CaO:xCr₂O₃ are selected for glass preparation, and in which 'x' changes from 0 to 1 mol% with a step size of 0.2 mol%. Detailed chemical composition of the present series of glass tests are given as follows

Cr0.0	60SiO ₂ + 30Al ₂ O ₃ + 10.0 CaO : 0.0 Cr ₂ O ₃
Cr0.2	60SiO ₂ + 30Al ₂ O ₃ + 09.8 CaO : 0.2 Cr ₂ O ₃
Cr0.4	60SiO ₂ + 30Al ₂ O ₃ + 09.6 CaO : 0.4 Cr ₂ O ₃
Cr0.6	60SiO ₂ + 30Al ₂ O ₃ + 09.4 CaO : 0.6 Cr ₂ O ₃
Cr0.8	60SiO ₂ + 30Al ₂ O ₃ + 09.2 CaO : 0.8 Cr ₂ O ₃
Cr1.0	60SiO ₂ + 30Al ₂ O ₃ + 09.0 CaO : 1.0 Cr ₂ O ₃

The AR grade 99% pure Ca, Al, Si, O and Cr oxide powder chemicals in appropriate ratios are grinded in an agate mortar for synthesis by the melt quenching technique. Finely mixed powders

of chemicals are taken in a crucible of volume 25ml, for melting with the help of programmed furnace. And melting temperature identified around at 1475–1490 °C. The bubble-free final transparent melt was discharged on brass cast for glass formation. Thereafter, the muffle furnace was used for annealing. This was done at 475 °C for 12 hours. The samples developed are dimensionally arranged and well refined for various characterisations such as structure, thermoluminescence, and electrical studies. Dimensionally arranged glass samples were used for various characterizations. Scale tech weighing balance is used to record mass of the samples. Mass of the glasses recorded with the help of Scale Tech digital weighing balance with a precision of 10^{-4} gm/cm³. Archimedes' principle was used to calculate the density values employing known weights of the glasses. Shimadzu XRD-7000 is used record X-ray diffraction patterns of the samples. Hitachi S 3700N is used to record the chemical analysis of the samples. Ultrasonic velocities, which will be helpful to evaluate all elastic measurements of glasses, are recorded with the help of a WT 311 D flaw detector with a precision of ± 10 m/s. Optical absorption spectra of glasses recorded with the help of V 670 Model, UV VIS NIR Spectrometer with a precision of 0.1 nm. Photoluminescence spectra of glasses recorded with the help of JASCO FP 6300 Spectrometer. MS Office 2007, Origin 8.5, MAT Lab 2.3, and Chem Draw Ultra 12.0 software used to analyse the results.

3. Results, and Discussion

3.1 Physical Properties

The physical properties of $60\text{SiO}_2+30\text{Al}_2\text{O}_3+(10-x)\text{CaO}+(x)\text{Cr}_2\text{O}_3$ glasses are reported. The reported glass 0.8 mol% Cr_2O_3 concentration being best among all the values of various physical quantities of all series of glasses. All the results concerning the physical properties of the glasses provide facts regarding the covalent structure of glasses. Archimedes' equity was employed to estimate mass of the samples, and the following equations [11] are used to evaluate the physical properties of glasses.

Density of a glass (D) = $\{(S_a)/(S_a - S_b)\} \times D_{\text{oxy}}$

Where, S_a - weight of a glass measured in air;

S_b - weight of glass measured in liquid ortho xylene;

D_{oxy} - density of ortho xylene.

The following equations [12,13] are used to evaluate all the physical properties of glasses.

Molar volume (V_m) = M/D ;

Ion concentration (N_i) = $N_A C(\rho)/M_w$

Ionic radius (R_i) = $1/(N_i)^{1/3}$

Polaron Radius (R_p) = $1/2 \{\pi/(6 N_i)\}^{1/3}$

Field Strength (F_i) = (Z/ R_p^2)

Electronegativity (χ_{th}) = $\sum_k A^k B^k$

Optical basicity (Λ_{th}) = $(75)/(\chi_{\text{th}}-1.35)$

Oxygen packing density (OPD) = $[(1000 * C * D)/(V_m)]$;

Where, M_w - weight of a glass measured in air;

Z - atomic number;

A^k - concentration of oxide compounds;

B^k - Pauling electronegativity of oxide compounds;

The observed average molecular weight increases and the density (ρ) decreases for the prepared glasses with increasing concentration of Cr_2O_3 . The calculated ionic concentration (N_i), field strength (F_i) and molar volume (V_m) increase with increasing concentration of Cr_2O_3 , whereas the corresponding ionic radius (r_i) and the polaron radius (r_p) decreases. The electronegativity (χ_{th}) of the prepared glasses calculated by using Pauling scale were found to decrease, whereas the observed theoretical optical basicity (Λ_{th}) increases. The calculated refractive index (μ), Polarizability (α) and molar refraction (R_m) decreases. The decrease in density of glasses is an indication of decreasing structural compactness or rigidity with the increase in the concentration of Cr_2O_3 due to the depolymerisation of glass samples.

Table 1. Physical properties of $60SiO_2+30Al_2O_3+(10-x)CaO+(x)Cr_2O_3$ glasses.

Glass	Cr ₀	Cr ₂	Cr ₄	Cr ₆	Cr ₈	Cr ₁₀
Density (gm/cm ³)	2.789	2.887	2.934	2.995	3.11	3.045
Ionic concentration (x10 ²⁰)	5.711	11.574	17.669	24.391	29.762
Ionic radius (Å)	12.053	9.5244	8.2717	7.4289	6.952
Polaron radius (Å)	4.8564	3.8377	3.3329	2.9933	2.8012
Molar volume (x 10 ¹⁴ cm ³ mol ⁻¹)	4.24	6.79	9.0023	11.161	12.744
Field strength (x 10 ¹⁴ cm ⁻²)	22.76	22.06	21.77	21.39	20.66	21.16
Oxygen Packing Density	84.836	85.488	86.139	86.598	87.439	88.088
Electronegativity	9.900	9.899	9.898	9.897	9.896	9.891
Optical Basicity	8.7719	8.7729	8.7739	8.7750	8.7760	8.7755
Refractive index	1.635	1.675	1.681	1.692	1.733	1.715

Table 1 reports the summary on physical properties of the glasses. The observed changes in density and molar volume of glasses were explained by understanding the structural changes that happened in the environment of different structural units of polyhedral of silicate, and aluminium cations due to calcium and chromium ions. The decrease in density of glasses is an indication of decreasing structural compactness or rigidity with the increase in the concentration of Cr_2O_3 due to the depolymerisation of glass samples. The magnitude of optical basicity indicates the ionic or covalent nature of glass, because of accumulated basicity suggests diminishing covalence. Accumulation of Cr_2O_3 interchanges the CaO, which affects in diminishing of magnitude of NBO's, the existing cage average charge around Cr^{3+} rises, relative molar volume increases, the Cr-O detachment increases up to 0.8 mol% afterwards decreases. The intensification of the manganese ions generally exists in Cr^{3+} states, occupy network forming positions with CrO_4 structural entities rise the rigidity of the glasses. Fig.1 reports the X-ray diffraction recording of one of the glasses with 0.8 mol% Cr_2O_3 concentration. The analysis suggests glassy behaviour of the sample. In same view, the results of the other glasses also observed.

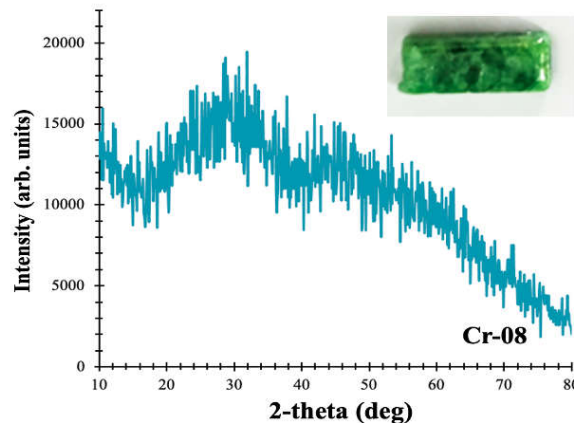


Fig. 1 X-Ray diffraction pattern of sample of glass with 0.8 mol% Cr_2O_3 concentration. Inset of the figure represent $60\text{SiO}_2+30\text{Al}_2\text{O}_3+(10-x)\text{CaO}+(x)\text{Cr}_2\text{O}_3$ series of glasses. Where 'x' varies 0 to 1 mol% with a step size of 0.2 mol%. The diffraction angles are taken up to an accuracy of $\pm 0.1^\circ$. lines drawn back ground of image only for better view of eye guiding.

3.2 Mechanical Properties

The succeeding equivalences are utilised to calculate several elastic constraints of the glass samples. Elastic behaviour, of the $60\text{SiO}_2+30\text{Al}_2\text{O}_3+(10-x)\text{CaO}+(x)\text{Cr}_2\text{O}_3$ glasses are carried. The poisson ratio, elastic (young, bulk, and shear) modulus, and micro-hardness of glasses are estimated. Up to 0.8 mol% Cr_2O_3 concentration the density, micro-hardness and elastic (young, bulk, and shear) modulus of the glasses are improved, after that they are in reverse trend. Fig.2 and 3 reports the variations in elastic parameters with increasing concentration of Cr_2O_3 . All these elastic properties of glasses evaluated by using following equations [14,15].

$$\text{Longitudinal elastic coefficient (L)} = D(Z_x)^2,$$

$$\text{Shear modulus (B)} = D(Z_y)^2,$$

$$\text{Bulk modulus (C)} = L - (4/3)B,$$

$$\text{Young's modulus (A)} = 2(1 + P)B,$$

$$\text{Poisson's ratio (P)} = \frac{1}{2}[(L - 2B)/(L - B)]$$

$$\text{Micro hardness } (\Omega) = (A/6)[(1 - 2P)/(1 + P)]$$

Where, S_1 – longitudinal velocity, and S_2 – shear velocity. The evaluated all the information with regard to mechanical properties of the $60\text{SiO}_2+30\text{Al}_2\text{O}_3+(10-x)\text{CaO}+(x)\text{Cr}_2\text{O}_3$ glasses presented in table number 02. Naturally, the glasses are extreme elastic behavior under any attentive glass formation. And the numerous elastic modulus of glass materials is an interdependent allocation of intermolecular control.

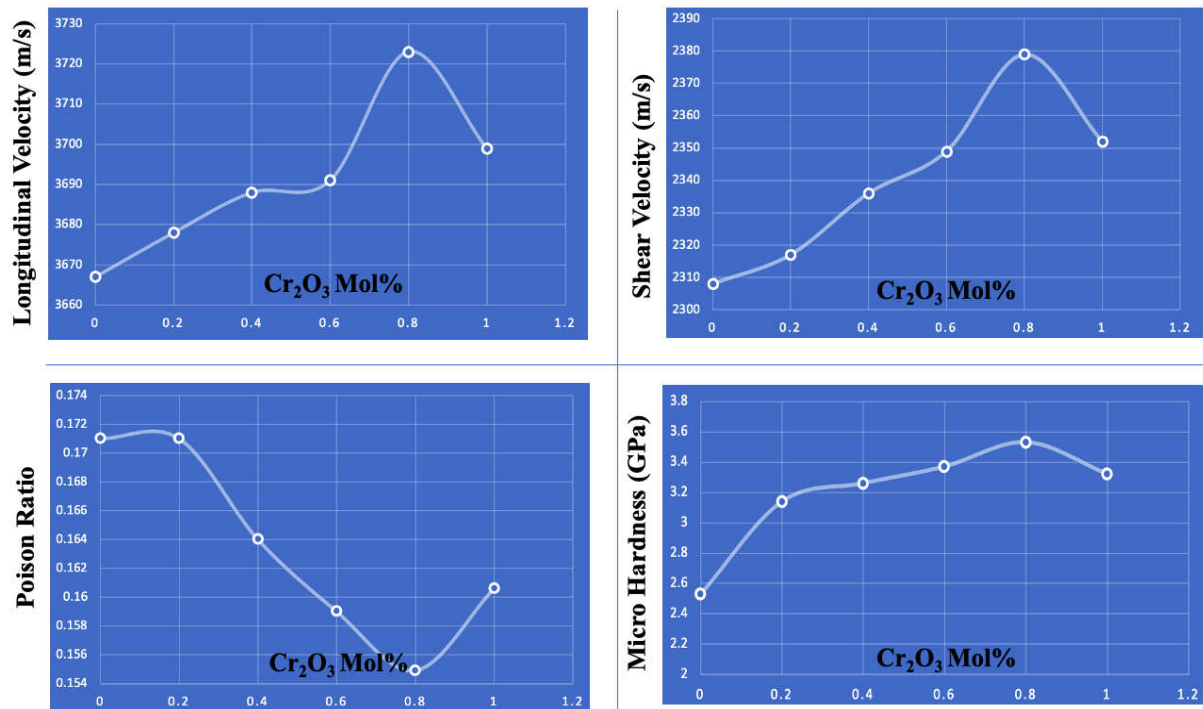


Fig. 2 Elastic properties: variation in (a) ultrasonic longitudinal velocity, (b) ultrasonic transverse velocity, (c) Poison ratio, and (d) micro hardness with Cr₂O₃ concentration 60SiO₂+30Al₂O₃+(10-x)CaO+(x)Cr₂O₃ series of glass materials where 'x' varies 0 to 1 mol% with a step size of 0.2 mol%.

In some glass (or) glass-ceramic materials, the elastic module improves through a predictable degree of molecular density. Replacement of Ca²⁺ ions by divalent Cr³⁺ ions within materials causes higher orders of variations in elastic modulus (bulk, shear, and young's).

Table 2. Mechanical properties of 60SiO₂+30Al₂O₃+(10-x)CaO+(x)Cr₂O₃ glasses.

Glass	Cr ₀	Cr ₂	Cr ₄	Cr ₆	Cr ₈	Cr ₁₀
Longitudinal velocity (Z _x) m/s	3667	3678	3688	3691	3723	3699
Transverse velocity (Z _y) m/s	2308	2317	2336	2349	2379	2352
Young's modulus (GPa)	27.20	33.58	34.10	34.53	35.50	34.08
Shear modulus (GPa)	11.60	14.33	14.63	14.89	15.37	14.68
Bulk modulus (GPa)	29.30	36.13	36.47	36.76	37.64	36.31
Poison Ratio (GPa)	0.171	0.171	0.164	0.159	0.1549	0.1606
Micro-hardness (GPa)	2.53	3.14	3.26	3.37	3.53	3.32

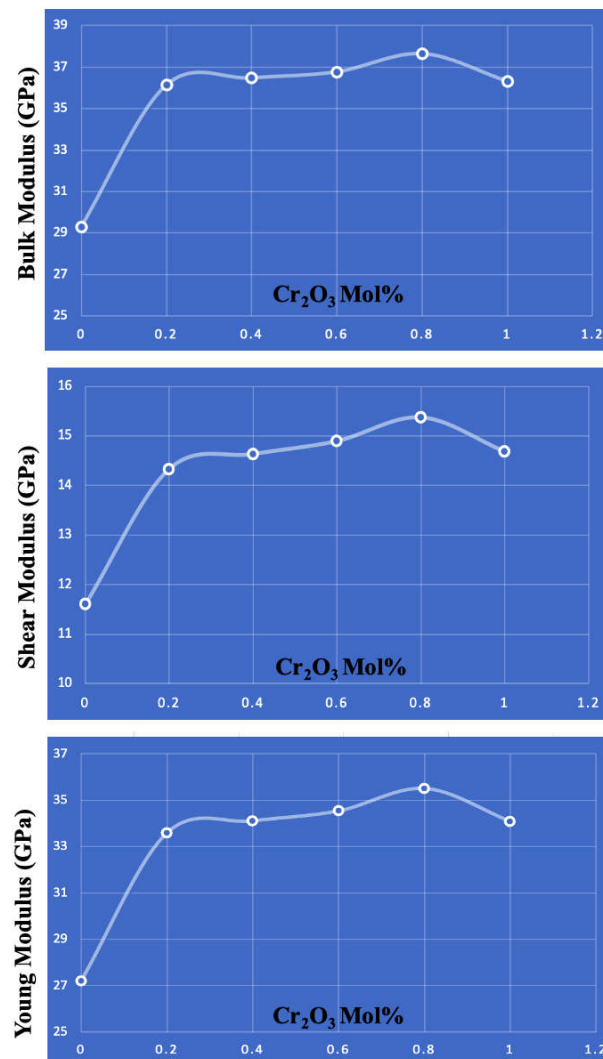


Fig. 3 Elastic properties: variation in (a) Young's modulus, (b) shear modulus, and (c) bulk modulus with Cr₂O₃ concentration 60SiO₂+30Al₂O₃+(10-x)CaO+(x)Cr₂O₃ series of glass materials, where 'x' varies 0 to 1 mol% with a step size of 0.2 mol%.

Further, which leads to a high degree of covalent bonding within a glass of 0.8 mol% Cr₂O₃ concentration, increased atomic density, and variations in interstitial defects could be another reason for increasing the bulk, shear, and young's module [16]. The Microhardness of present glasses prescribes additional information about covalently interlinked structure.

3.3 Spectroscopic Properties

3.3.1 Optical Absorption

Fig. 4 reports the optical absorption of current glasses. And the OBE of glasses found at ~ 285.7 nm. Glass code with 0.8 mol% Cr₂O₃ concentration observed to be highest among all the values of the present series of materials. Analysis reveal Cr₂O₃ absorption bands such as transitions

${}^4A_{2g}(F) \rightarrow {}^4T_{1g}(F)$, ${}^4A_{2g}(F) \rightarrow {}^4T_{2g}(F)$, ${}^4A_{2g}(F) \rightarrow {}^2E_g$ and ${}^4A_{2g}(F) \rightarrow {}^2T_{1g}(G)$ around at 456–466 nm, 618–629 nm, 667–675 nm and 695–703 nm wavelength range [17-20]]. Fig.5 reports Tauc plots of glasses, which will help to find band gap's values of glasses. In this view, the glass with 0.8 mol% Cr_2O_3 concentration observed to be highest among all other glasses. Urbach energy evaluations are also reported and analysed for a better description of glasses. From the different observed transitions of optical absorption spectra of present glass ceramics, the crystal field splitting energy (D_q), Racah (B,C) parameters and nephelauxetic ratio (β) were calculated by following equations.

$$D_q = \{E({}^4A_{2g}) - E({}^4T_{1g})\} / 10$$

$$D_q/B = 15(X-8)/(X^2-10X)$$

$$X = \{E[{}^4A_{2g}(F) \rightarrow {}^2T_{1g}(G)] - E[{}^4A_{2g}(F) \rightarrow {}^4T_{2g}(F)]\} / D_q$$

$$10D_q + 4B + 3C = E[{}^4A_{2g}(F) \rightarrow {}^2A_{1g}(G)]$$

The decrease in value of nephelauxetic ratio (β) indicates that the decrease in covalence with in these glass ceramic materials with increase in concentration of Cr_2O_3 . Absorption spectra evaluations, identifications, and results of current $60SiO_2+30Al_2O_3+(10-x)CaO+(x)Cr_2O_3$ glasses reported in table number 03. The observed optical absorption spectra and Tauc plots of $60SiO_2+30Al_2O_3+(10-x)CaO+(x)Cr_2O_3$ added with Cr_2O_3 glass materials were reveal, the parameter optical band gap decrease with increase in the content of Cr_2O_3 . This is due to number of non-bridging oxygen's (NBO's) and bond defects increase with in the glass ceramic network and these further cause depolymerisation of glass ceramics network by Cr^{3+} ions along with Ba^{2+} ions.

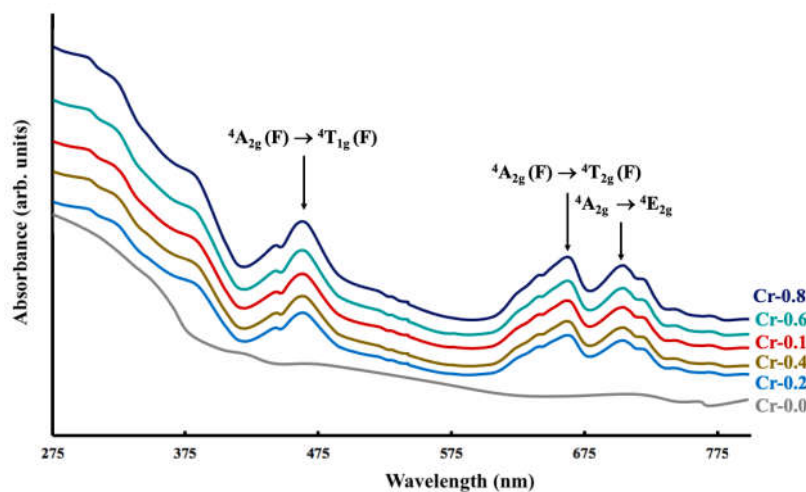


Fig. 4 Optical absorption spectra of $60SiO_2+30Al_2O_3+(10-x)CaO+(x)Cr_2O_3$ series of glass materials recorded at room temperature with in the wavelength range of 200 - 800 nm range. The wavelengths are taken up to an accuracy of ± 0.1 nm and Mac based MATLAB 2.3 version to plot the figure.

The addition of Cr_2O_3 up to 01 mol% within the glass ceramic network leads to increase in Cr^{3+} ions cause formation of different donor ions tends to overlap with excited states of electrons. These different reasons reveal the impurity energy band spreads into the original band gap leads

decrease in optical band gap.

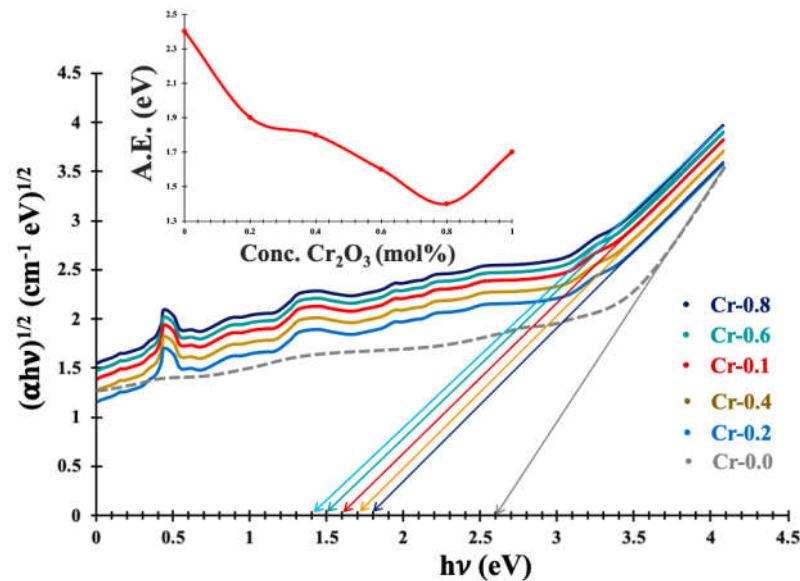


Fig. 5 Tauc plots of $60\text{SiO}_2+30\text{Al}_2\text{O}_3+(10-x)\text{CaO}+(x)\text{Cr}_2\text{O}_3$ series of glass materials. Where 'x' varies 0 to 1 mol% with a step size of 0.2 mol%. Wavelengths are taken up to an accuracy of ± 0.1 nm.

Table 3. Summary on optical absorption of $60\text{SiO}_2+30\text{Al}_2\text{O}_3+(10-x)\text{CaO}+(x)\text{Cr}_2\text{O}_3$ glass materials recorded at room temperature.

Glass	Cr ₀	Cr ₂	Cr ₄	Cr ₆	Cr ₈	Cr ₁₀
Band edge(nm)	259.5	261	263	266.7	270	268
Optical band gap E_o (eV)	2.65	1.8	1.7	1.6	1.4	1.5
Urbach Energy ΔE (eV)	0.361	0.379	0.395	0.415	0.435	0.429
$^4A_{2g}(F) \rightarrow ^4T_{1g}(F)$ (nm)	---	453	455	459	466	463
$^4A_{2g}(F) \rightarrow ^4T_{2g}(F)$ (nm)	---	623	625	628	632	629
$^4A_{2g}(F) \rightarrow ^2E_{2g}(F)$ (nm)	---	692	694	697	704	701
CFSC D_q (cm^{-1})	---	1475	1481	1493	1499	1495
Racah parameter B (cm^{-1})	---	851	854	864	869	862
Racah parameter C (cm^{-1})	---	2781	2792	2999	3051	3023
nephelauxetic ratio	---	0.834	0.847	0.869	0.885	0.876

3.3.2 Photoluminescence

Fig.6 reports photoluminescence of glasses. Luminescence parameters such as cross-section, transition probability analogous to the emissive band $^4T_{2g}(F) \rightarrow ^4A_{2g}(F)$ around at 650 –661 nm. wavelength range are evaluated and analysed. The glass with 0.8 mol% Cr_2O_3 concentration observed to be highest among all the values of various luminescent quantities of glasses. The subsequent equations are used [21,23] to determine luminescence results

$$A = [8v^2 \times 10^6] / (e)^2;$$

$$\delta = [(\lambda)^4 A] / [8\pi\Delta\lambda c (\mu)^2];$$

Where, λ -wavelength; $\Delta\lambda$ - peak half width; A- transition probability; μ -refractive index; δ - cross section; v - frequency; c - velocity of light; e - electron charge; Fig.7 indicates the colour Chromacity report of glass with 0.8 mol% Cr₂O₃ concentration.

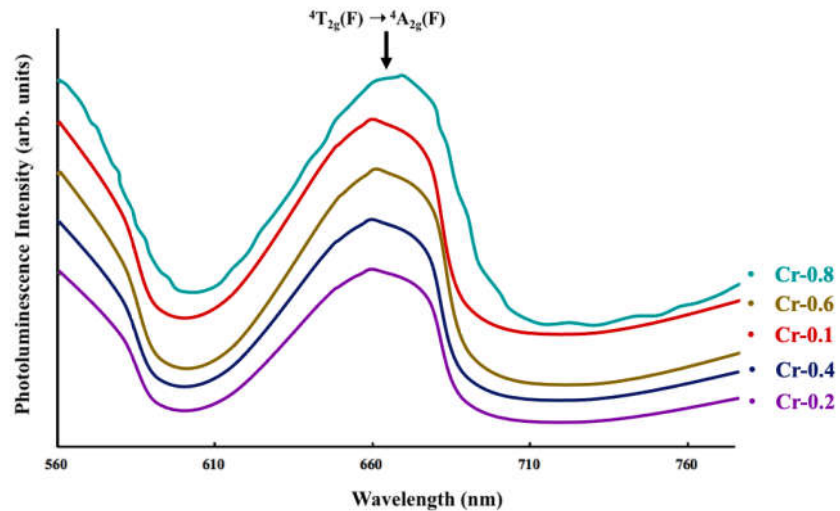


Fig.6 Photoluminescence spectra of 60SiO₂+30Al₂O₃+(10-x)CaO+(x)Cr₂O₃ series of glass materials recorded at room temperature with in the wavelength range of 370 to 800 nm and with an excitation wavelengths of both 361 nm. The wavelengths are taken up to an accuracy of ± 0.1 nm.

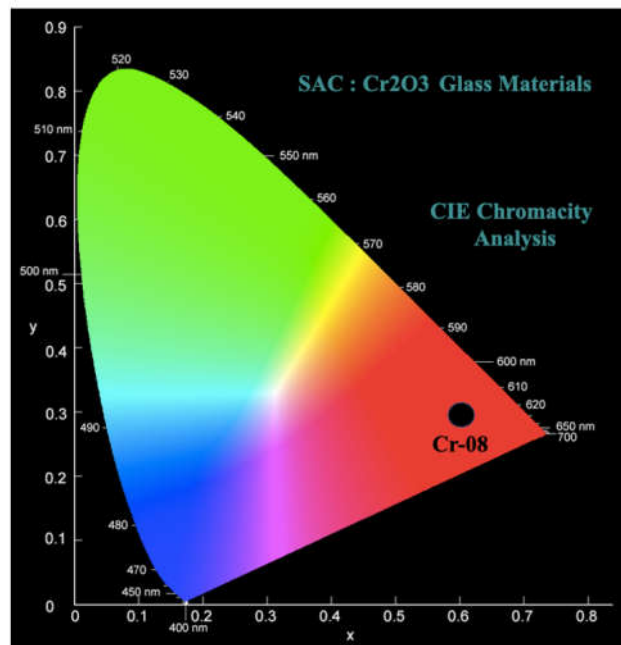


Fig.7 Chromacity analysis of $60\text{SiO}_2+30\text{Al}_2\text{O}_3+(10-x)\text{CaO}+(x)\text{Cr}_2\text{O}_3$ series of glass materials, where 'x' varies 0 to 1 mol% with a step size of 0.2 mol%. The wavelengths are taken up to an accuracy of ± 0.1 nm and Mac based MATLAB 2.3 version to plot the figure.

All the photoluminescence results of current $60\text{SiO}_2+30\text{Al}_2\text{O}_3+(10-x)\text{CaO}+(x)\text{Cr}_2\text{O}_3$ glasses reported in table number 04. The Chromacity analysis relative to transition ${}^4\text{T}_{2g}(\text{F}) \rightarrow {}^4\text{A}_{2g}(\text{F})$ suggests orange emission. However, it is changing with Cr_2O_3 concentration [24,25]. In this view, the glass code 0.8 mol% Cr_2O_3 concentration observe to exhibit the highest shift towards the red region among all the values of the present series of materials. Improved efficiency up to 0.8 mol% Cr_2O_3 concentration intensity is due to an enlarged number of octahedral Cr^{3+} ions within the glasses. The Luminescence spectra of present glass samples were exhibited the transition ${}^4\text{T}_{2g}(\text{F}) \rightarrow {}^4\text{A}_{2g}(\text{F})$ (octahedral positioned Cr^{3+} ions) around at 660 nm. With increase in the content of Cr_2O_3 there is increasing in intensity of emission band. The red shift up to 0.8 mol% of Cr_2O_3 with in these glass ceramic samples is due to sharp fall in the strength of crystal field surrounding Cr^{3+} ions. Which cause the reduction in the difference between ground state and excited state. The enhanced photoluminescence with in these glass ceramic materials with increase in concentration of Cr_2O_3 due to octahedrally occupied Cr^{3+} ions.

Table 4. Data on photoluminescence spectra of $60\text{SiO}_2+30\text{Al}_2\text{O}_3+(10-x)\text{CaO}+(x)\text{Cr}_2\text{O}_3$ glass materials recorded at room temperature.

Glass	Emission peak position (nm) ${}^4\text{T}_{2g}(\text{F}) \rightarrow {}^4\text{A}_{2g}(\text{F})$	Peak half width ($\Delta\lambda$)	Transition probability ($\times 10^{34}$)	Emission cross-section ($\times 10^{11}$, cm^2)
Cr ₂	653	40	0.922	0.331
Cr ₄	655	39	0.929	0.369
Cr ₆	657	37	0.936	0.397
Cr ₈	661	31	0.941	0.435
Cr ₁₀	659	33	0.935	0.421

4. Conclusion

In the present work, we have synthesized the $60\text{SiO}_2+30\text{Al}_2\text{O}_3+(10-x)\text{CaO}+(x)\text{Cr}_2\text{O}_3$ glasses, where 'x' varies with a step size 0.2 mol % from 0 to 1.0 mol %. The structure of the glasses studied by means of X-ray diffraction. Under Physical Studies, evaluated density, molar volume, optical basicity, polaronic strength and optical basicity of the glasses found to be highest for a glass with 0.8 mol% Cr_2O_3 concentration, which suggests higher order of intermolecular force and covalence in between Cr^{3+} ions to all other Ca^{2+} , Al^{3+} and Si^{4+} ions in a glass with 0.8 mol% Cr_2O_3 concentration. Ultrasonic velocities are recorded to evaluate the elastic characteristics of glasses. Under elastic characterization, the evaluated microhardness (~ 3.53 GPa) range suggests higher rigidity and elastic strength of glasses. Refractive index (~ 1.733), Optical bandgap (~ 1.4 eV), transition probability ($\sim 0.941 \times 10^{34} \text{ S}^{-1}$) and cross-section ($\sim 0.941 \times 10^{11} \text{ cm}^2$) values analogous to the transition ${}^3\text{T}_1(\text{P}) \rightarrow {}^3\text{A}_2(\text{F})$ of glass with 0.8 mol% Cr_2O_3 concentration is a highly suggestable glass for photonic use. Based on structure, physical, mechanical and

spectroscopic studies of glasses recommend that glass with 0.8 mol% Cr₂O₃ concentration is a desirable resource for thermoluminescent use.

Conflicts of Interest

Declare None

Authors Contribution Statement

- Mr. Kodumuri Veerabhadra Rao– methodology, characterization, analysis, and report writing.
- Mr. Padala. Ashok – conceptualization, methodology, characterization, analysis, report drafting.
- Dr. B. Appara Rao – report correction, and suggestions

Acknowledgments

The authors thank Management of Methodist College of Engineering and Technology, ABIDS, Hyderabad – 500 001, Telangana, INDIA for continuous moral support during the overall task.

Reference

1. M.S. Gaafar, S.Y. Marzouk, I.S. Mahmoud, Role of dysprosium on some acoustic and physical properties of PbO-B₂O₃-SiO₂ glasses, Results in Physics, Volume 22, 2021, 103944, ISSN 2211- 3797, <https://doi.org/10.1016/j.rinp.2021.103944>.
2. Jia-Jun He, Shao-Yi Wu, Li-Juan Zhang, Yong-Qiang Xu, Chang-Chun Ding, Theoretical studies of the concentration dependences of g factor and d-d transition band for Cin CdO–SrO–B₂O₃–SiO₂ glasses, Journal of Non-Crystalline Solids, Volume 437, 2016, Pages 58-63, ISSN 0022-3093, <https://doi.org/10.1016/j.jnoncrysol.2016.01.019>.
3. Ravi Kumar Guntu, Nd₂O₃ Influenced Al₂O₃ & Sb₂O₃ Functional PbO-SiO₂ Glass, Materials, 1.06 μm Photonic Resource, Materials Science and Engineering: B, Volume 262, 2020, 114784, ISSN 0921-5107, <https://doi.org/10.1016/j.mseb.2020.114784>.
4. Byeongwon Park, Hong Li, L.René Corrales, Molecular dynamics simulation of La₂O₃–Na₂O–SiO₂ glasses. I. The structural role of La³⁺cations, Journal of Non-Crystalline Solids, Volume 297, Issues 2–3, 2002, Pages 220-238, ISSN 0022-3093, [https://doi.org/10.1016/S0022-3093\(01\)00935-8](https://doi.org/10.1016/S0022-3093(01)00935-8).
5. Hirokazu Masai, Go Okada, Noriaki Kawaguchi, Takayuki Yanagida, Photoluminescence and X- ray-induced scintillation of BaO-TiO₂-SiO₂ glasses and the glass-ceramics, Journal of Non- Crystalline Solids, Volume 501, 2018, Pages 131-135, ISSN 0022-3093, <https://doi.org/10.1016/j.jnoncrysol.2017.11.026>.
6. Fabien Pacaud, Mathieu Salanne, Thibault Charpentier, Laurent Cormier, Jean-Marc Delaye, Structural study of Na₂O-B₂O₃-SiO₂-La₂O₃ glasses from molecular simulations using a polarizable force field, Journal of Non-Crystalline Solids, Volume 499, 2018, Pages 371-379, ISSN 0022-3093, <https://doi.org/10.1016/j.jnoncrysol.2018.07.049>.

7. Maha Rai, Gavin Mountjoy, Molecular dynamics modelling of the structure of barium silicate glasses BaO–SiO₂, Journal of Non-Crystalline Solids, Volume 401, 2014, Pages 159-163, ISSN 0022-3093, <https://doi.org/10.1016/j.jnoncrysol.2013.12.026>.
8. P. Goharian, B. Eftekhari Yekta, A.R. Aghaei, S. Banijamali, Lithium ion-conducting glass-ceramics in the system Li₂O–TiO₂–P₂O₅–Cr₂O₃–SiO₂, Journal of Non-Crystalline Solids, Volume 409, 2015, Pages 120-125, ISSN 0022-3093, <https://doi.org/10.1016/j.jnoncrysol.2014.11.016>.
9. Taoyong Liu, Cui Li, Qianxing Huang, Chenxing Liu, Changwei Lin, Qian Zhang, Zhiwei Luo, Ligang Zhu, Anxian Lu, Characterization of structure and properties of MgO-Al₂O₃-SiO₂-B₂O₃-Cr₂O₃ glass-ceramics, Journal of Non-Crystalline Solids, Volume 543, 2020, 120154, ISSN 0022-3093, <https://doi.org/10.1016/j.jnoncrysol.2020.120154>.
10. Stelian Pintea, Vasile Rednic, Petru Mărginean, Nicolae Aldea, Hu Tiandou, Zhonghua Wu, Manfred Neumann, Florica Matei, Crystalline and electronic structure of Ni nanoclusters supported on Al₂O₃ and Cr₂O₃ investigated by XRD, XAS and XPS methods, Superlattices and Microstructures, Volume 46, Issues 1–2, 2009, Pages 130-136, ISSN 0749-6036, <https://doi.org/10.1016/j.spmi.2009.01.003>.
11. Takashi Wakasugi, Takuya Kadoguchi, Rikuo Ota, Evaluation of the number density of nuclei in Li₂O·2SiO₂ glass by DTA method, Journal of Non-Crystalline Solids, Volume 290, Issue 1, 2001, Pages 64-72, ISSN 0022-3093, [https://doi.org/10.1016/S0022-3093\(01\)00718-9](https://doi.org/10.1016/S0022-3093(01)00718-9).
12. G. Ravi Kumar, M.C. Rao, Structural and photoluminescence investigations of Cr³⁺ mixed Li₂O–Bi₂O₃–ZrO₂–SiO₂ glass ceramics for optoelectronic device application, Optik, Volume 181, 2019, Pages 721-731, ISSN 0030-4026, <https://doi.org/10.1016/j.ijleo.2018.12.110>.
13. B. Mirhadi, B. Mehdikhani, Crystallization behavior and microstructure of (CaO·ZrO₂·SiO₂)–Cr₂O₃ based glasses, Journal of Non-Crystalline Solids, Volume 357, Issues 22–23, 2011, Pages 3711-3716, ISSN 0022-3093, <https://doi.org/10.1016/j.jnoncrysol.2011.07.040>.
14. Ravi Kumar Guntu*, 'Elastic, thermoluminescence and dielectric characterization of lead antimony silicate glass composites doped by small concentrations of Cr₂O₃', Bulletin Material Science, Volume 42, 2019, 214, ISSN 0250-4707, <https://doi.org/10.1007/s12034-019-1892-3>.
15. G. Ravi Kumar, M. Gopi Krishna, M.C. Rao, 'Cr³⁺ doped NaF–ZrO₂–B₂O₃–SiO₂ glass-ceramic materials for optoelectronic device application', Optik, Volume 173, 2018, Pages 78-87, ISSN 0030-4026, <https://doi.org/10.1016/j.ijleo.2018.07.114>.
16. Vijay Singh, R.P.S. Chakradhar, J.L. Rao, S.H. Kim, EPR and luminescence studies of Cr³⁺ doped MgSrAl₁₀O₁₇ phosphor synthesized by a low-temperature solution combustion

- route, Journal of Luminescence, Volume 154, 2014, Pages 328-333, ISSN 0022-2313, <https://doi.org/10.1016/j.jlumin.2014.03.035>.
17. F.S. De Vicente, F.A. Santos, B.S. Simões, S.T. Dias, M. Siu Li, EPR, optical absorption and luminescence studies of Cr³⁺-doped antimony phosphate glasses, Optical Materials, Volume 38, 2014, Pages 119-125, ISSN 0925-3467, <https://doi.org/10.1016/j.optmat.2014.10.012>.
 18. M.I. Sayyed, H.O. Tekin, O. Agar, Gamma photon and neutron attenuation properties of MgO–BaO– B₂O₃–TeO₂–Cr₂O₃ glasses: The role of TeO₂, Radiation Physics and Chemistry, Volume 163, 2019, Pages 58-66, ISSN 0969-806X, <https://doi.org/10.1016/j.radphyschem.2019.05.012>.
 19. G. Ravi Kumar, M. Gopi Krishna, M.C. Rao, Cr³⁺-doped NaF–ZrO₂–B₂O₃–SiO₂ glass ceramic materials for optoelectronic device application, Optik, Volume 173, 2018, Pages 78-87, ISSN 0030- 4026, <https://doi.org/10.1016/j.ijleo.2018.07.114>.
 20. G. Ravi Kumar, M.C. Rao, Structural and photoluminescence investigations of Cr³⁺ mixed Li₂O— Bi₂O₃—ZrO₂—SiO₂ glass ceramics for optoelectronic device application, Optik, Volume 181, 2019, Pages 721-731, ISSN 0030-4026, <https://doi.org/10.1016/j.ijleo.2018.12.110>.
 21. B.K. Sudhakar, N.R.K. Chand, H.N.L. Prasanna, G. Srinivasa Rao, K. Venkateswara Rao, Vivek Dhand, Vibrational spectral analysis of structural modifications of Cr₂O₃ containing oxyfluoroborate glasses, Journal of Non-Crystalline Solids, Volume 356, Issue 43, 2010, Pages 2211-2217, ISSN 0022-3093, <https://doi.org/10.1016/j.jnoncrysol.2010.08.034>.
 22. Jau-Sheng Wang, Feng-Hsi Shen, The development of SiO₂ resistant Cr-doped glass ceramics for high Cr³⁺-emission, Journal of Non-Crystalline Solids, Volume 358, Issue 2, 2012, Pages 246-251, ISSN 0022-3093, <https://doi.org/10.1016/j.jnoncrysol.2011.09.022>.
 23. G. Susoy, E.E. Altunsoy Guclu, Ozge Kilicoglu, M. Kamislioglu, M.S. Al-Buriah, M.M. Abuzaid, H.O. Tekin, The impact of Cr₂O₃ additive on nuclear radiation shielding properties of LiF–SrO– B₂O₃ glass system, Materials Chemistry and Physics, Volume 242, 2020, 122481, ISSN 0254-0584 <https://doi.org/10.1016/j.matchemphys.2019.122481>.
 24. A. Ramesh Babu, S. Yusub, P.M. Vinaya Teja, P. Srinivasa Rao, V. Aruna, D. Krishna Rao, Effect of Cr₂O₃ on the structural, optical and dielectric studies of LiF–SrO–B₂O₃ glasses, Journal of Non-Crystalline Solids, Volume 520, 2019, 119428, ISSN 0022-3093, <https://doi.org/10.1016/j.jnoncrysol.2019.05.004>.
 25. B. Srinivas, B. Srikantha Chary, Abdul Hameed, M. Narasimha Chary, Md. Shareefuddin, Influence of BaO on spectral studies of Cr₂O₃ doped titanium-boro-tellurite glasses, Optical Materials, Volume 109, 2020, 110329, ISSN 0925-3467, <https://doi.org/10.1016/j.optmat.2020.110329>.